

Thermodynamic properties of tetrameric bond-alternating spin chains

H. T. Lu,^{1,2} Y. H. Su,³ L. Q. Sun,² J. Chang,² C. S. Liu,² H. G. Luo,² and T. Xiang²

¹*School of Physics, Peking University, Beijing 100871, China*

²*Institute of Theoretical Physics and Interdisciplinary Center of Theoretical Studies, Chinese Academy of Sciences, Beijing 100080, China*

³*Center for Advanced Study, Tsinghua University, Beijing 100084, China*

(Received 17 December 2004; published 29 April 2005)

Thermodynamic properties of a tetrameric bond-alternating Heisenberg spin chain with ferromagnetic-ferromagnetic-antiferromagnetic-antiferromagnetic exchange interactions are studied using the transfer-matrix renormalization group and compared to experimental measurements. The temperature dependence of the uniform susceptibility exhibits typical ferrimagnetic features. Both the uniform and staggered magnetic susceptibilities diverge in the limit $T \rightarrow 0$, indicating that the ground state has both ferromagnetic and antiferromagnetic long-range orders. A double-peak structure appears in the temperature dependence of the specific heat. Our numerical calculation gives a good account for the temperature and field dependence of the susceptibility, the magnetization, and the specific heat for $\text{Cu}(\text{3-Clpy})_2(\text{N}_3)_2$ (3-Clpy=3-Chloropyridine).

DOI: 10.1103/PhysRevB.71.144426

PACS number(s): 75.10.Jm, 05.50.+q

I. INTRODUCTION

Physical properties of one-dimensional quantum ferrimagnets have attracted much interest in recent years. In particular, physical properties of the so-called Lieb-Mattis¹-type ferrimagnets have been extensively investigated both theoretically and experimentally.²⁻⁵ In these materials, there exists strong competition between ferromagnetic and antiferromagnetic fluctuations. This competition leads to a ferrimagnetic-ordered ground state with coexisting gapless ferromagnetic and gapped antiferromagnetic excitations, a minimum in the temperature dependence of the product of the susceptibility and temperature, a double-peak structure in the specific heat, and a wide variety of other physical phenomena.

A Lieb-Mattis-type ferrimagnet can be constructed from monospin chains with polymerized exchange interactions. It can be also constructed from an alternating spin chain with antiferromagnetic interactions. These two types of ferrimagnets are equivalent to each other in certain limits. Many of their thermodynamic or dynamic response functions show qualitatively similar behaviors. For convenience in the discussion below, we call the ferrimagnets formed from monospins or from alternating large and small spins as Type-I or Type-II ferrimagnets.

The simplest bond-alternating spin chain is a ferromagnetic-antiferromagnetic (F-AF) alternating Heisenberg spin chain. A typical example of this F-AF alternating spin chain is the compound $(\text{CH}_3)_2\text{CHNH}_3\text{CuCl}_3$. Manaka *et al.*⁶ did birefringence measurement on this material. Although the ground state of the compound is nondegenerate, a double-peak structure of the specific heat was observed.

A Type-I ferrimagnet can be constructed from a tetrameric ferromagnetic-ferromagnetic-antiferromagnetic-antiferromagnetic (F-F-AF-AF) Heisenberg exchange spin chain. Recently, Hagiwara *et al.* studied thermodynamic properties^{7,8} of a tetrameric chain compound $\text{Cu}(\text{3-Clpy})_2(\text{N}_3)_2$ (3-Clpy=3-Chloropyridine), abbreviated as

CCPA below.⁹ Typical behavior of ferrimagnets was revealed. Furthermore, by exactly diagonalizing an isotropic F-F-AF-AF Heisenberg model on small lattice, they found that the experimental data for the magnetization and susceptibility can be quantitatively understood from this model.^{7,8} There were also other theoretical and numerical studies on this tetrameric chain system. Yamamoto calculated the zero-field specific heat and susceptibility of the F-F-AF-AF Heisenberg model using the modified spin-wave theory as well as the Quantum Monte Carlo method.¹⁰ Nakanishi and Yamamoto¹¹ found that the specific heat of this model shows a double-peak structure. However, a direct comparison between experiments and numerical calculations, especially for the temperature dependence of the specific heat, is still absent.

A typical Type-II ferrimagnet is the alternating $S=1$ and $1/2$ spin chain. Kahn's group¹² synthesized successfully a class of bimetallic chain compounds with each unit cell containing two spins with different values. Typical compounds include $\text{ACu}(\text{pba})(\text{H}_2\text{O})_3 \cdot n\text{H}_2\text{O}$ and $\text{ACu}(\text{pbaOH})(\text{H}_2\text{O})_3 \cdot n\text{H}_2\text{O}$, where $\text{A}=\text{Mn}, \text{Fe}, \text{Co}, \text{Ni}, \text{Zn}$, $\text{pba}=1,3\text{-propylenebis (oxamato)}$, and $\text{pbaOH}=2\text{-hydroxy-1, 3-propylenebis(oxamato)}$. This has stimulated theoretical studies on alternating spin chains. From numerical simulations, Pati *et al.*² revealed the coexistence of gapless and gapped excitations in alternating spin-(1,1/2) ferrimagnetic chains using the density-matrix renormalization group (DMRG).¹³ The coexistence of ferromagnetic and antiferromagnetic aspects was also found by Brehmer *et al.*¹⁴ from quantum Monte Carlo (QMC) simulations. Thermodynamic properties of the alternating spin chains were studied by the transfer-matrix renormalization group (TMRG).⁴ To further explore the dual features of ferrimagnetism, the Schwinger boson and the spin-wave approximations were exploited.^{4,5,10}

In this paper, we investigate numerically thermodynamic properties of tetrameric spin chains with alternating F-F-AF-AF exchange interactions and compare the results to

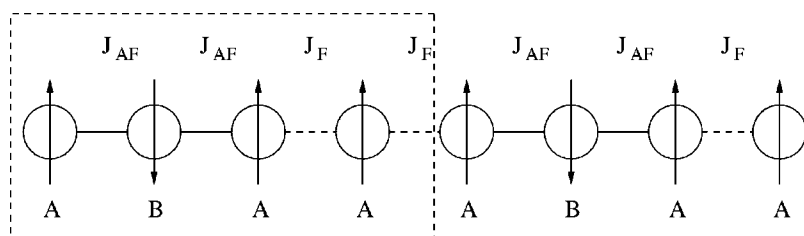


FIG. 1. Schematic representation of the chain structure of $\text{Cu}(\text{3-Clpy})_2(\text{N}_3)_2$ (CCPA) with interactions described by Hamiltonian (1). The system can be decomposed into two sublattices according to the nature of coupling, i.e., A and B sublattices, respectively.

the experimental data for CCPA. In Sec. II, the isotropic F-F-AF-AF Heisenberg exchange model for the tetrameric spin chains with its general properties is introduced. In Sec. III, thermodynamic quantities of the tetrameric model including the magnetization, uniform and staggered magnetic susceptibilities, and field-dependent specific heat, are evaluated using the transfer-matrix renormalization group.¹⁵⁻¹⁷ Section IV compares the numerical results to the experimental data on CCPA. Our numerical results agree well with the experimental data for the zero-field uniform susceptibility as well as the magnetization. The numerical results for the difference of the specific heat between two different fields are also in good agreement with the experimental data. We briefly discuss the sharp low-temperature peak that appeared in the zero-field specific-heat curve published in Refs. 7 and 8. It is suggested that this experimental sharp peak is an extrinsic feature and most probably because of the contribution of magnetic impurities.

II. MODEL HAMILTONIAN AND GENERAL PROPERTIES

CCPA is a tetrameric spin-chain compound. It consists of copper chains in which adjacent Cu^{2+} ions are linked by two kinds of azido bridges, namely, end-on and end-to-end bridge, respectively [Fig. 1 of Ref. 7]. The exchange interactions between adjacent Cu^{2+} ions are determined by the azido bridges linked to them. The low-energy magnetic excitations in this material can be modeled by a $S=1/2$ Heisenberg Hamiltonian defined by

$$H = H_0 + H', \quad (1)$$

$$H_0 = \sum_{i=1}^L [J_F \mathbf{S}_{4i-3} \cdot \mathbf{S}_{4i-2} + J_{AF} \mathbf{S}_{4i-2} \cdot \mathbf{S}_{4i-1} + J_{AF} \mathbf{S}_{4i-1} \cdot \mathbf{S}_{4i} + J_F \mathbf{S}_{4i} \cdot \mathbf{S}_{4i+1}], \quad (2)$$

$$H' = - \sum_{i=1}^{4L} g \mu_B h S_i^z, \quad (3)$$

where L is the number of unit cells, J_F and J_{AF} are the ferromagnetic and antiferromagnetic exchange constants, respectively, g is the magnetic g factor, and h is the external magnetic field. This model belongs to the family of Lieb-Mattis-type ferrimagnets, as shown in Fig. 1.

According to the Lieb-Mattis theorem,¹ this tetrameric system has $(2L+1)$ -fold degenerate ground states with total spin $S_{\text{tot}}=L$. The macroscopic magnetization of the ground state has been quantitatively confirmed by magnetization measurements with pulsed and static fields on a single crystal of CCPA.⁸

In the limit $J_F=0$, the system is decoupled into isolated trimers, separated by local one-half spins. The Hamiltonian then becomes

$$H = \sum_{i=1}^L H_i^{(c)}, \quad (4)$$

where

$$H_i^{(c)} = J_{AF} (\mathbf{S}_{4i-2} \cdot \mathbf{S}_{4i-1} + \mathbf{S}_{4i-1} \cdot \mathbf{S}_{4i}) - g \mu_B h (S_{4i-3}^z + S_{4i-2}^z + S_{4i-1}^z + S_{4i}^z). \quad (5)$$

This model is exactly soluble. In the absence of an applied field, an antiferromagnetic trimer is a three-level system with a doubly degenerate ground state of $S_{\text{tot}}=1/2$. One excited state is twofold degenerate with $S_{\text{tot}}=1/2$ and an energy J_{AF} above the ground state. The other is fourfold degenerate with $S_{\text{tot}}=3/2$ and an energy $3J_{AF}/2$ above the ground state. For finite but small J_F , the ferromagnetic correlation dominates the low-temperature excitations. The low-temperature behavior of the system is expected to act similarly as a spin- $1/2$ ferromagnetic spin chain.

In the limit $|J_F| \gg J_{AF}$, the three ferromagnetically coupled neighbors in one unit will bind together to form a $3/2$ spin. In this case, the system is expected to behave similarly as a $(S, s)=(3/2, 1/2)$ Heisenberg ferrimagnetic spin chain.

For the alternating $(S, s)=(1, 1/2)$ Heisenberg spin chain,^{2,4,5,14} there exist both gapless ferromagnetic and gapped antiferromagnetic excitations. For the bond-alternating ferrimagnetic spin chain considered here, these two kinds of excitations are also expected to exist. In low temperatures, thermodynamic properties of the system are more strongly affected by ferromagnetic excitations. However, with increasing temperatures, the contribution from gapped antiferromagnetic excitations increases. This leads to a crossover in the behavior of C and χ . For instance, in low temperatures, for the $(S, s)=(1, 1/2)$ spin chains, the specific heat and the susceptibility vary respectively as $C \propto T^{1/2}$ and $\chi \propto T^{-2}$, same as for the spin- $1/2$ ferromagnetic spin chain. However, in the intermediate temperature regime, they show a Schottky-like peak and a minimum, respectively.⁴

III. NUMERICAL RESULTS

In this section, we will use the TMRG to evaluate the temperature dependence of the magnetic susceptibility and the specific heat for the tetrameric bond-alternating spin model described by Hamiltonian (1). The TMRG is a powerful numerical tool for studying thermodynamic properties of one-dimensional quantum systems.¹⁵⁻¹⁷ It starts by ex-

pressing the partition function of a one-dimensional quantum lattice system as a trace of a virtual transfer matrix \tilde{T}_M using the Trotter-Suzuki decomposition

$$Z = \text{Tr} e^{-\beta H} = \lim_{M \rightarrow \infty} \text{Tr} \tilde{T}_M^{N/2}, \quad (6)$$

where M is the Trotter number, N is the system size, and $\tau = \beta/M$. For the tetrameric model considered here, $N=2L$ and each site used in the Trotter-Suzuki decomposition contains two spins. In the limit $N \rightarrow \infty$, one can evaluate nearly all thermodynamic quantities by the maximum eigenvalue λ_{\max} and the corresponding left $\langle \psi^L |$ and right $|\psi^R \rangle$ eigenvectors of the transfer matrix \tilde{T}_M . For example, the free energy F , internal energy U , and longitudinal magnetization M_z per unit cell can be expressed, respectively, as

$$F = - \lim_{N \rightarrow \infty} \frac{1}{N\beta} \ln Z = - \frac{1}{2\beta} \lim_{M \rightarrow \infty} \ln \lambda_{\max}, \quad (7)$$

$$U = \frac{\langle \psi^L | \tilde{T}_U | \psi^R \rangle}{\lambda_{\max}}, \quad (8)$$

$$M_z = \frac{\langle \psi^L | \tilde{T}_M | \psi^R \rangle}{\lambda_{\max}}, \quad (9)$$

where the definition of the transfer matrices \tilde{T}_U and \tilde{T}_M can be found from Refs. 16 and 17. The specific heat and magnetic susceptibility can then be calculated by numerical derivatives of U and M_z , respectively,

$$C = \frac{\partial U}{\partial T}, \quad (10)$$

$$\chi = \frac{\partial M_z}{\partial H}. \quad (11)$$

In our TMRG iterations, 60 states are retained in the calculation of the susceptibility, and 80 states are retained in the calculation of the specific heat. The error results from the Trotter-Suzuki decomposition is less than 10^{-3} . The truncation errors are smaller than 10^{-8} .

Figure 2 shows the temperature dependence of the uniform zero-field susceptibility multiplied by temperature χT . When $J_F=0$, χT approaches a finite value in the limit $T \rightarrow 0$, in agreement with the Curie-Weiss law for a free magnetic moment of $S=1/2$. With increasing temperature, excitations corresponding to higher spins in the trimers are stimulated and χT increases and saturates in high temperatures. For finite J_F , χT diverges in the limit $T \rightarrow 0$, because of the formation of ferromagnetic long-range order in the ground state. Generally, χT decreases monotonically with temperature for ferromagnets, whereas it increases monotonically with temperature for antiferromagnets. The behavior of χT for this ferrimagnet reflects the interplay of these two opposite trends. Gapless ferromagnetic excitations reduce the magnetization at low T , while thermally activated antiferromagnetic excitations give rise to the increase of χT at high T . The presence of a minimum in χT for all nonzero J_F is a typical feature of one-dimensional (1D) ferrimagnets.

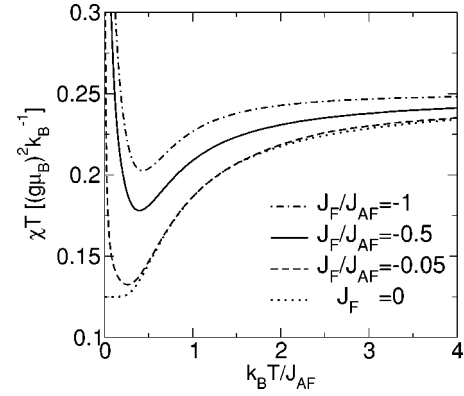


FIG. 2. TMRG results (except for the case $J_F=0$) of the uniform zero-field susceptibility multiplied by temperature for the tetrameric bond-alternating spin model.

Similar behavior was observed in the alternating $(S, s) = (1, 1/2)$ spin chain.⁴ This minimum moves slightly toward higher temperature with increasing $|J_F|/J_{AF}$, resulting from the enhancement of ferromagnetic correlations.

Figure 3 shows the temperature dependence of the staggered susceptibility. To calculate the staggered susceptibility, we add a staggered magnetic field h_s instead of a uniform field to the Hamiltonian. Two kinds of staggered fields are considered. One is a staggered-field applied to the whole lattice. The corresponding Zeeman interaction, staggered magnetization, and susceptibility are defined by

$$H_s^{(1)} = -g\mu_B h_s \sum_{i=1}^{2L} (S_{2i-1}^z - S_{2i}^z), \quad (12)$$

$$M_s^{(1)} = \frac{g\mu_B}{4L} \sum_{i=1}^{2L} \langle S_{2i-1}^z - S_{2i}^z \rangle, \quad (13)$$

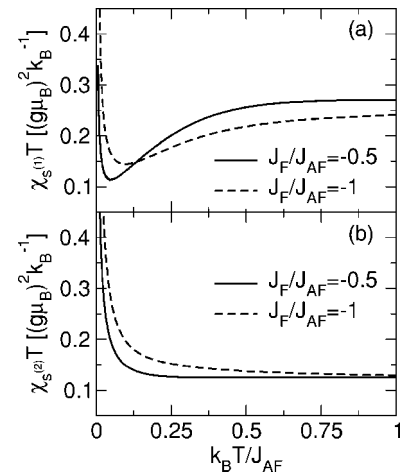


FIG. 3. The zero-field staggered susceptibilities multiplied by temperature. $\chi_s^{(1)}$ and $\chi_s^{(2)}$ are defined by Eqs. (14) and (17), respectively.

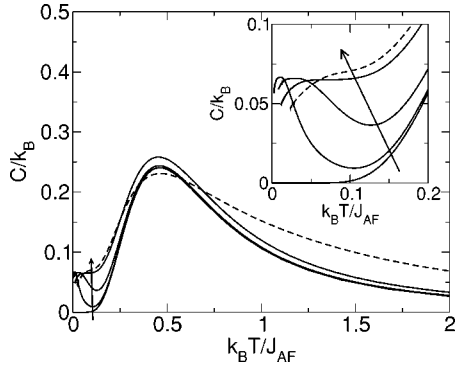


FIG. 4. TMRG results of the zero-field specific heat at $|J_F|/J_{AF}=0, 0.05, 0.15, 0.5, 2.0$ in ascending order along the direction of arrows. The case $|J_F|/J_{AF}=2.0$ is plotted as a dashed line for visual effect. The inset shows the low-temperature part of the specific heat.

$$\chi_s^{(1)} = \frac{\partial M_s^{(1)}}{\partial h_s}. \quad (14)$$

The staggered susceptibility $\chi_s^{(1)}$ as defined corresponds to the spin structure factor at $q=\pi$. Another kind of staggered field we consider is that applied only to the first and third spins in each unit cell. The corresponding Zeeman interaction, staggered magnetization, and susceptibility are defined by

$$H_s^{(2)} = - \sum_{i=1}^L g\mu_B h_s (S_{4i-3}^z - S_{4i-1}^z), \quad (15)$$

$$M_s^{(2)} = \frac{g\mu_B}{4L} \sum_{i=1}^L \langle S_{4i-3}^z - S_{4i-1}^z \rangle, \quad (16)$$

$$\chi_s^{(2)} = \frac{\partial M_s^{(2)}}{\partial h_s}. \quad (17)$$

$\chi_s^{(2)}$ corresponds to a sum of the spin structure factor at $q = \pm\pi/2$. As revealed by Fig. 3, both staggered susceptibilities, $M_s^{(1)}$ and $M_s^{(2)}$, diverge at $T=0$ in the zero-field limit.

The divergence of the uniform susceptibility χ as well as the two staggered susceptibilities $\chi_s^{(1)}$ and $\chi_s^{(2)}$ is an indication of the formation of ferromagnetic as well as antiferromagnetic long-range orders at zero temperature. This is consistent with a rigorous theorem about the ferromagnetic and antiferromagnetic orders in the ground state of Type-II ferrimagnets.¹⁸

Figure 4 shows the temperature dependence of the zero-field specific heat at different J_F/J_{AF} . When $J_F=0$, the specific heat drops quickly in low temperatures because of the finite-energy gap between the ground state and excitation states. At finite J_F , a small peak develops in low temperatures and C shows a small peak-valley structure. The low-temperature peak of C results from the gapless ferromagnetic excitations, as illustrated by Fig. 5. In low temperatures, the temperature dependence of C/T measures the energy dependence of the density of states of low-lying ferromagnetic

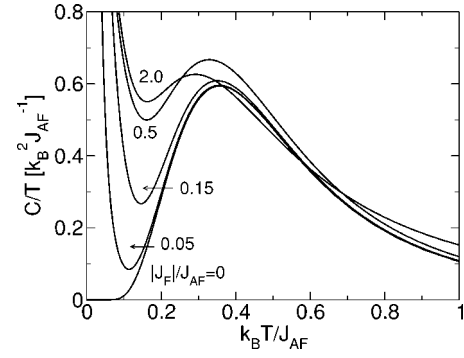


FIG. 5. The zero-field specific heat coefficient C/T versus T for $|J_F|/J_{AF}=0, 0.05, 0.15, 0.5, 2.0$.

excitations. For finite J_F , since the density of states of ferromagnetic excitations diverges at zero energy, C/T is expected to diverge at $T=0$ K. For $|J_F|/J_{AF} \geq 0.5$, as shown by Fig. 4, the small peak-valley in the low-temperature specific heat changes gradually into a hump structure. A more conspicuous peak around $k_B T \sim 0.5 J_{AF}$ exists in all the cases studied. This broadened peak, often called the Schottky-like peak, is associated with gapped antiferromagnetic excitations, as predicted by various methods^{2,4,5,14} for the Lieb-Mattis-type ferrimagnets.

The double-peak structure of the specific heat for ferrimagnets was also observed by Nakanishi and Yamamoto¹¹ using modified spin-wave theory. They found that this double-peak structure of the zero-field specific heat is an intrinsic feature with topological origin, since the dual features of ferromagnetism and antiferromagnetism in ferrimagnets can potentially induce a low-temperature peak as well as an intermediate-temperature peak. They calculated the low-lying spectra of the tetrameric chain. Three bands of ferromagnetic excitations with one gapless and two gapped, and one band of gapped antiferromagnetic excitation were found. From the above qualitative analysis on the F-F-AF-AF model, we believe that in the region $|J_F| \ll J_{AF}$, the low-energy physics of the tetrameric chain is governed by the ferromagnetic coupling. In this region, the peak should move to higher temperature with increasing $|J_F|$. Our numerical results support the above arguments. The positions and the heights of the low-temperature peaks in the calculations are consistent with the results for the $S=1/2$ Heisenberg model with the same ferromagnetic interaction J_F . With increasing $|J_F|$, we find that the peak moves toward higher temperature and eventually mixes with other excitations, leading to a hump structure. However, the position and the height of the Schottky-like peak are not sensitive to the ratio $|J_F|/J_{AF}$. This is different to the modified-spin-wave theory.¹¹ It should be emphasized that the intrinsic double-peak structure of the specific heat is not a distinctive character of bond-alternating-type ferrimagnets. As pointed out by Nakanishi and Yamamoto,¹¹ this structure appears when the antiferromagnetic gap is larger than the ferromagnetic bandwidth. For the (S, s) alternating-spin-type ferrimagnets, this condition is satisfied for $S \gg s$.

At finite magnetic field, due to the field-induced splitting of ferromagnetic excitations, a double-peak structure of the

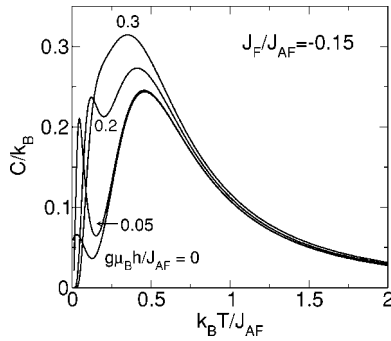


FIG. 6. Temperature dependence of the specific heat for $J_F/J_{AF} = -0.15$ at different external magnetic fields.

specific heat can also appear in some ferrimagnets, such as for the case $(S, s) = (1, 1/2)$.¹⁹ However, these two cases should be clearly distinguished. Figure 6 shows the temperature dependence of the specific heat for $J_F/J_{AF} = -0.15$ at different external fields. When a weak field is applied, C shows a sharp low-temperature peak. With increasing field, the double-peak structure is smeared out and merges together, due to the Zeeman splitting.¹⁹ The Zeeman splitting of the eigenvalues leads to a finite energy gap in the ferromagnetic excitations proportional to h , but reduces the energy gap in the antiferromagnetic excitations.

Recently, Strečka *et al.*^{20,21} investigated thermodynamic properties of a spin- $\frac{1}{2}$ Ising-Heisenberg chain with F-F-AF-AF bond-alternating interaction using a mapping-transformation technique. They considered the Ising-type ferromagnetic interaction. Nevertheless, their results agree qualitatively with ours.

IV. COMPARISON TO EXPERIMENTS

In this part we calculate the susceptibility and specific heat of the tetrameric model in the parameter regime relevant to CCPA and compare the numerical results to the experimental data published in Refs. 7 and 8.

A. Magnetization and susceptibility

Figure 7 compares the TMRG results of $\chi(T)T$ for different J_F/J_{AF} to the experimental data for CCPA. The parameters used are the same as in Ref. 7. A good agreement between experiments and calculations is found when $J_F/J_{AF} \approx -0.6$, same as in Ref. 7. However, above 70 K, the numerical curves are slightly below the experimental ones.

Figure 8 compares the TMRG results of the field dependence of the longitudinal magnetization to the experimental data. Within experimental errors, the TMRG results agree with the experiments in the low-field regime. In the high-field regime, the numerical curve deviates slightly from the experimental data. It is unknown whether this deviation is because of some unknown effects or measurement errors. At $T = 1.7$ K, there is a broad magnetization plateau. This plateau is a typical feature of a quantum ferrimagnet, due to macroscopic magnetization of the ground state. At relatively high temperature $T = 4.2$ K, the plateau region shows a weak

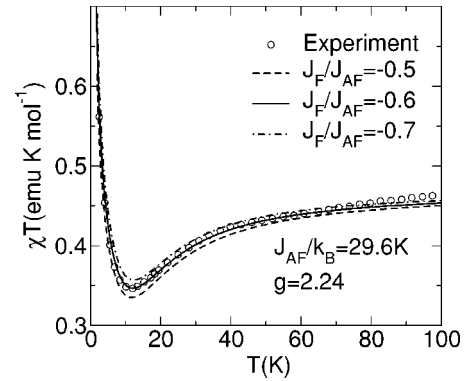


FIG. 7. Comparison between our numerical results for the magnetic susceptibility multiplied by temperature and the experimental data published in Ref. 7.

field dependence resulting from thermal fluctuations.

At high fields, the magnetization increases sharply and becomes saturated for $T = 1.7$ K. At $T = 4.2$ K, the magnetization curve is smoothed by thermal fluctuations. In the work of Strečka *et al.*,^{20,21} quantum fluctuations are restricted to the antiferromagnetic trimers since the ferromagnetic coupling is Ising-like. A stepwise increase of magnetization with B at very low temperature is expected because of the short correlation length inherent in this quantum ferrimagnet. Nakanishi and Yamamoto calculated the spectrum of the F-F-AF-AF Heisenberg model using the modified-spin wave.¹¹ They found that in the region $|J_F/J_{AF}| < 1$, the antiferromagnetic excitations are almost dispersionless. It is this dispersionless antiferromagnetic excitation that enhances the magnetization. The above comparison suggests that the F-F-AF-AF Heisenberg model can describe quantitatively the temperature dependence of the susceptibility and field dependence of the magnetization of CCPA with $J_F/J_{AF} \sim -0.6$.

B. Specific heat

Figure 9 shows the numerical results on the temperature dependence of the specific heat $C(T)$ at different fields for

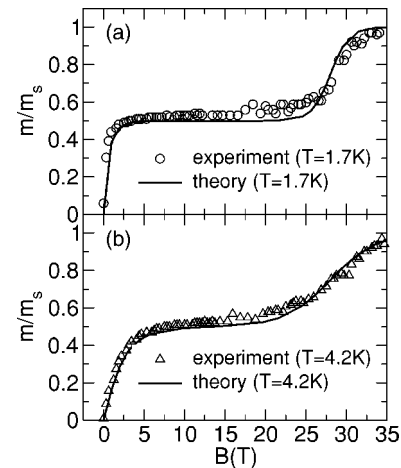


FIG. 8. Comparison of the measured experimental data of the field dependence of low-temperature longitudinal magnetization⁸ to the TMRG results. The parameters used are $J_{AF}/k_B = 29.6$ K, $J_F/J_{AF} = -0.6$, $g = 2.24$. m_s is the saturation magnetization.

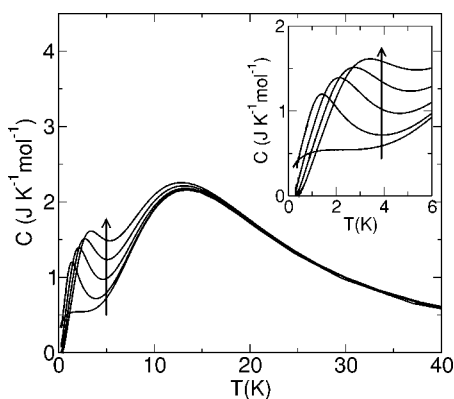


FIG. 9. TMRG results for the temperature dependence of the specific heat at $H=0, 0.5, 1.0, 1.5, 2.0$ T in ascending order along the direction of arrows. The parameters used are the same as for Fig. 8. The inset shows the low-temperature part of C .

$J_F/J_{AF} = -0.6$. At zero field, C increases in a certain power law of T in low temperatures. When an external field is applied, a double-peak structure appears. With increasing H , the low-temperature peak moves toward higher temperature, but the high-temperature peak moves in the opposite direction.

Figure 10 compares the experimental data of C to our numerical calculations. At finite fields, the numerical results agree well with the experimental data below 3 K. However, in relatively higher temperatures, the experimental curves are clearly above the numerical ones.

The experimental data shown in Fig. 10 were obtained from the measurement raw data by subtracting the T^3 phonon contribution to the specific heat. This subtraction may not always be accurate. Thus we have reason to suspect that the deviation at high temperatures may come from the error in the subtraction of the phonon contribution.

In order to reduce the error in the data subtraction, we compare our numerical results of the difference of the specific heat at a finite field and that at zero field, ΔC_1

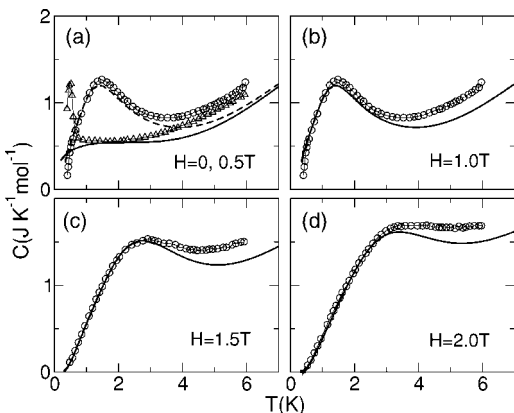


FIG. 10. Comparison of the specific heat of CCPA to the TMRG results. In (a) the triangle (solid), circle (dashed) lines represent the experimental (numerical) data for $H=0, 0.5$ T, respectively; In (b), (c), (d), the circle and solid lines represent experimental and numerical results, respectively. The parameters used are the same as for Fig. 8.

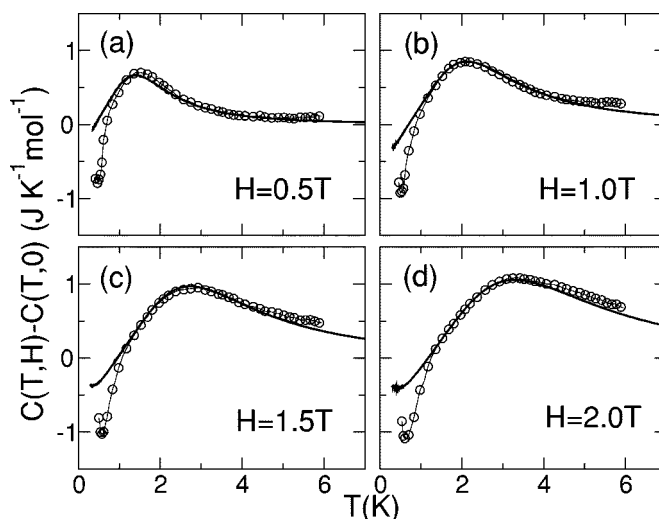


FIG. 11. Comparison of the specific heat of CCPA to TMRG results after subtracting the corresponding zero-field data. Circles and solid lines represent experimental and numerical results, respectively. The parameters are the same as for Fig. 8.

$= C(T, H) - C(T, 0)$, to the corresponding experimental data. As shown in Fig. 11, the agreement between the experimental and numerical results is improved, especially in high T , from 1.3 K to 6 K. However, in low temperatures, the agreement became worse. This is clearly because of the presence of the experimental sharp peak around 0.5 K at zero magnetic field.

Hagiwara *et al.*⁷ suggested that when a Heisenberg spin chain has more than two kinds of exchange interactions, the specific heat is expected to show more than one peak. Manaka *et al.*⁶ also found the double-peak structure in the temperature dependence of the specific heat by the birefringence measurements in ferromagnetic-dominant F-AF alternating Heisenberg chains $(\text{CH}_3)_2\text{CHNH}_3\text{CuCl}_3$. From Sec. III, we know that the intrinsic double-peak structure of the specific heat for the Heisenberg F-F-AF-AF model could be observed when $|J_F|/J_{AF}$ is small enough. But for the given parameter $J_F/J_{AF} = -0.6$, the sharp peak at 0.5 K is not expected. Strečka *et al.*²¹ also made a comparison of theoretical results on the F-F-AF-AF Ising-Heisenberg model with experiments. In order to fit the striking low-temperature peak around 0.5 K, $|J_F|/J_{AF}$ had to be drastically reduced, and the results merely qualitatively agreed with experiments. On the other hand, from the experimental data, the experimental sharp peak around 0.5 K seems to be suppressed by magnetic field [Fig. 4 in Ref. 7]. The behavior is different from the usual situation, as shown in Fig. 6, where the low-temperature peak of the double-peak structure is strengthened by a weak external field.

We believe that the experimental sharp peak of the specific heat around 0.5 K at zero magnetic field is not an intrinsic property of the model. It may result from some extrinsic properties of the material, such as defects or boundary states. Further measurements and more extensive theoretical and numerical analysis are needed for fully understanding this behavior.

To avoid the contribution from the experimental sharp low-temperature peak of the specific heat at zero field, we

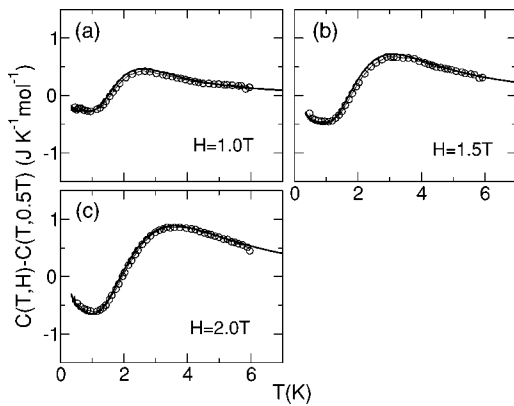


FIG. 12. Comparison of the specific heat of CCPA to TMRG results after subtracting the corresponding data at $H=0.5$ T. Circles and solid lines represent experimental and numerical results, respectively. The parameters are the same as for Fig. 8.

show in Fig. 12 the results for $\Delta C_2 = C(T, H) - C(T, 0.5 \text{ T})$, which subtracts the data in the field $H=0.5$ T, instead of at zero field. We find that our numerical results agree excellently with the experiments. This indicates that the experimental sharp low-temperature peak of the zero-field specific heat is indeed extrinsic.

V. CONCLUSION

We have investigated numerically thermodynamic properties of the bond-alternating F-F-AF-AF tetramer Heisenberg spin chain using the TMRG. The temperature dependence of

the spin susceptibility and the specific heat is found to be determined by the competition of gapless ferromagnetic excitations and gapped antiferromagnetic excitations. This leads to a crossover in the behavior of C and χ . With increasing temperature, χT drops sharply in low temperatures, but increases and becomes saturated in high temperatures. The minimum of χT increases gradually with increasing $|J_F/J_{AF}|$. Both the uniform and staggered susceptibilities diverge in the zero temperature limit. This suggests that both ferromagnetic and antiferromagnetic spin correlations are long-range ordered in the ground state. C shows a small peak in low temperatures and a stronger and broadened Schottky-like peak in an intermediate temperature regime. The nonmonotonic T dependence of χT and the double-peak structure of C are also the characteristic features of alternating spin ferrimagnets.

Our numerical results for the temperature dependence of χ and the difference of C between two different fields $C(H) - C(0.5 \text{ T})$ with $J_F/J_{AF} = -0.6$ agree excellently with the experimental data for CCPA. The field dependence of the magnetization agrees also with the experiment. We argue that the sharp peak observed at ~ 0.5 K in the zero-field specific heat is an extrinsic feature of CCPA. It is likely to be the contribution of defects or magnetic impurities. Further experimental measurements with high-quality samples are desired to clarify this issue.

ACKNOWLEDGMENT

This work was supported by the National Natural Science Foundation of China. Part of the numerical work of this project was performed on the HP-SC45 Sigma-X parallel computer of ITP and ICTS, CAS.

- ¹E. Lieb and D. Mattis, *J. Math. Phys.* **3**, 749 (1962).
- ²S. K. Pati, S. Ramasesha, and D. Sen, *Phys. Rev. B* **55**, 8894 (1997).
- ³S. Yamamoto, S. Brehmer, and H.-J. Mikeska, *Phys. Rev. B* **57**, 13610 (1998).
- ⁴S. Yamamoto, T. Fukui, K. Maisinger, and U. Schollwöck, *J. Phys.: Condens. Matter* **10**, 11033 (1998).
- ⁵C. Wu, B. Chen, X. Dai, Y. Yu, and Z.-B. Su, *Phys. Rev. B* **60**, 1057 (1999).
- ⁶H. Manaka, I. Yamada, T. Kikuchi, K. Morishita, and K. Iio, *J. Phys. Soc. Jpn.* **70**, 2509 (2001).
- ⁷M. Hagiwara, K. Minami, and H. A. Katori, *Prog. Theor. Phys. Suppl.* **145**, 150 (2002).
- ⁸M. Hagiwara, Y. Narumi, K. Minami, K. Kindo, H. Kitazawa, H. Suzuki, N. Tsujii, and H. Abe, *J. Phys. Soc. Jpn.* **72**, 943 (2003).
- ⁹A. Escuer, R. Vicente, M. S. El Fallah, M. A. S. Goher, and F. A. Mautner, *Inorg. Chem.* **37**, 4466 (1998).
- ¹⁰S. Yamamoto, *Phys. Rev. B* **69**, 064426 (2004).
- ¹¹T. Nakanishi and S. Yamamoto, *Phys. Rev. B* **65**, 214418 (2002).
- ¹²O. Kahn, *Struct. Bonding (Berlin)* **68**, 89 (1987); O. Kahn, Y.

- Pei, and Y. Journaux, in *Inorganic Materials*, edited by D. W. Bruce and D. O' Hare (Wiley, New York, 1995), p. 25.
- ¹³S. R. White, *Phys. Rev. Lett.* **69**, 2863 (1992).
- ¹⁴S. Brehmer, H.-J. Mikeska, and S. Yamamoto, *J. Phys.: Condens. Matter* **9**, 3921 (1997).
- ¹⁵R. J. Bursill, T. Xiang, and G. A. Gehring, *J. Phys.: Condens. Matter* **8**, L583 (1996).
- ¹⁶X. Wang and T. Xiang, *Phys. Rev. B* **56**, 5061 (1997).
- ¹⁷T. Xiang and X. Wang, in *Density-Matrix Renormalization: A New Numerical Method in Physics*, edited by I. Peschel, X. Wang, M. Kaulke, and K. Hallberg (Springer, New York, 1999), pp. 149–172.
- ¹⁸Guangshan Tian, *Phys. Rev. B* **56**, 5355 (1997).
- ¹⁹K. Maisinger, U. Schollwöck, S. Brehmer, H. J. Mikeska, and S. Yamamoto, *Phys. Rev. B* **58**, R5908 (1998).
- ²⁰J. Strečka, M. Jaščur, M. Hagiwara, and K. Minami, *Czech. J. Phys.* **54**, D583 (2004).
- ²¹J. Strečka, M. Jaščur, M. Hagiwara, Y. Narumi, K. Kindo, and K. Minami, cond-mat/0406680 (unpublished).